

1 Preparation of TFC Membranes Supported with Electrospun Nanofibers 2 for Desalination by Forward Osmosis

3 Mustafa Al-Furaiji^{1,*}, Mohammed Kadhom², Khairi Kalash¹, Basma Waisi³, Noor Albayati⁴

4 ¹ Environment and Water Directorate, Ministry of Science and Technology, Baghdad, Iraq

5 ² Department of Environment, College of Energy and Environmental Sciences, Alkarkh University of Science, Baghdad, Iraq

6 ³ Department of Chemical Engineering, College of Engineering, University of Baghdad, Baghdad, Iraq

7 ⁴ Department of Science, College of Basic Education, University of Wasit, Azizia, Wasit, Iraq

8 Corresponding Author: email: alfurajij79@gmail.com; phone: +964-7736-792-156

9 Abstract

10 The forward osmosis (FO) process has been considered as a viable option for water desalination in
11 comparison to the traditional processes like reverse osmosis, regarding energy consumption and
12 economical operation. In this work, polyacrylonitrile (PAN) nanofiber support layer was prepared using
13 the electrospinning process as a modern method. Then, an interfacial polymerization reaction between
14 m-phenylenediamine (MPD) and trimesoyl chloride (TMC) was carried out to generate a polyamide
15 selective thin film composite (TFC) membrane on the support layer. The TFC membrane was tested in
16 FO mode (feed solution facing the active layer) using the standard methodology and compared to a
17 commercially available cellulose triacetate membrane (CTA). The synthesized membrane showed a high
18 performance in terms of water flux ($16 \text{ Lm}^{-2}\text{h}^{-1}$) but traded the salt rejection ($4 \text{ gm}^{-2}\text{h}^{-1}$) comparing with
19 the commercially CTA membrane (water flux= $13 \text{ Lm}^{-2}\text{h}^{-1}$ and salt rejection= $3 \text{ gm}^{-2}\text{h}^{-1}$) at no applied
20 pressure and room temperature. Scanning electron microscopy (SEM), contact angle, mechanical
21 properties, porosity, and performance characterizations were conducted to examine the membrane.

22

23 **Keywords: Forward Osmosis; TFC membrane; Desalination; Nanofibers; Electrospinning**

24

1. Introduction

Forward osmosis is an osmotically-driven membrane process that uses the difference in osmotic pressure between the feed solution and a highly concentrated solution (called draw solution) to drive the pure water from feed solution through the membrane to the draw solution. The FO process has many advantages over other types of filtration processes, such as its low or no trans-pressure, very high rejection for various contaminants, low membrane fouling tendency, and easy building and operating system. The used system is very simple and membrane support is less of a problem (Al-Furaiji et al., 2018; Cath et al., 2006).

One of the crucial aspects of developing the FO process is making a suitable membrane for this process. The ideal membrane has to be highly porous, thin, owning good mechanical properties, and provides high rejection of salts and impurities (Ang et al., 2019). Thin-film composite (TFC) membranes have been widely used in reverse osmosis studies and proven to have excellent performance in desalination (Kadhom et al., 2016; Kadhom and Deng, 2019). Recently, TFC membranes have attracted more attention in FO applications.

Commonly, the TFC membranes consist of two layers: a thin selective film that permits water molecules to pass through but prevents salts and other contaminations, and a support layer that provides the required mechanical backing (Ren and McCutcheon, 2014). The selective thin layer is typically prepared by the interfacial polymerization reaction of *m*-phenylenediamine aqueous solution and 1,3,5-benzenetricarbonyl trichloride, which is familiarly called trimesoyl chloride, organic solution on the support layer. The support sheet is conventionally prepared by the phase inversion casting method. Here, we adopted an emerging technology, electrospinning, to prepare the support layer. Electrospinning has some advantages over the traditional phase inversion technique that include producing highly porous layers and generating sub-micron fibers with highly controllable properties (Waisi et al., 2019). These properties have led to introduce these nanofiber sheets as promising alternatives for the conventional FO membrane's support layers. Bui and McCutcheon 2013 investigated blending two kinds of polymer (i.e. PAN and cellulose acetate) to make hydrophilic nanofibers for FO applications (Bui and McCutcheon, 2013). Huang and McCutcheon used Nylon 6,6 electrospun nanofibers as support for TFC FO membranes

52 (Huang and McCutcheon, 2014). While Chowdhury et al. prepared and tested a TFC membrane supported
53 with commercial polyethersulfone (PES) nanofiber membranes (Chowdhury et al., 2017). All these
54 electrospun nanofibers based TFC membrane showed excellent performance over the commercial FO
55 membranes.

56 In this work, a thin-film composite polyamide membrane was synthesized by reacting MPD and TMC on
57 the electrospun PAN nanofibers support layer and utilized in the forward osmosis process. The
58 electrospun PAN nanofibers were prepared using a home-made electrospinning setup that was fabricated
59 from locally available parts; highly porous and highly efficient nanofibers were produced using a very
60 low-cost method. The membranes prepared in this study were mainly characterized by SEM and contact
61 angle to investigate the impact of the highly porous support layer, in addition to other tests. FO
62 experiments were carried out using a custom-built setup that utilize sodium chloride as a draw solution
63 for the process.

64 **2. Materials and Methods**

65 **2.1. Materials**

66 Polyacrylonitrile (PAN) of an average molecular weight of 150,000 was purchased from Macklin,
67 Shanghai, China. N, N dimethylformamide (DMF), and Isooctane were obtained from Fluka Chemie AG,
68 Buchs, Switzerland. The interfacial polymerization raw materials (*m*-phenylenediamine (>99%) and
69 trimesoyl chloride (98%)) were ordered from Merck. Sodium chloride (NaCl) was purchased from
70 Thomas Baker, India, while Polyethersulfone (PES) of M.wt. = 150,000 was purchased from Macklin
71 (Shanghai, China).

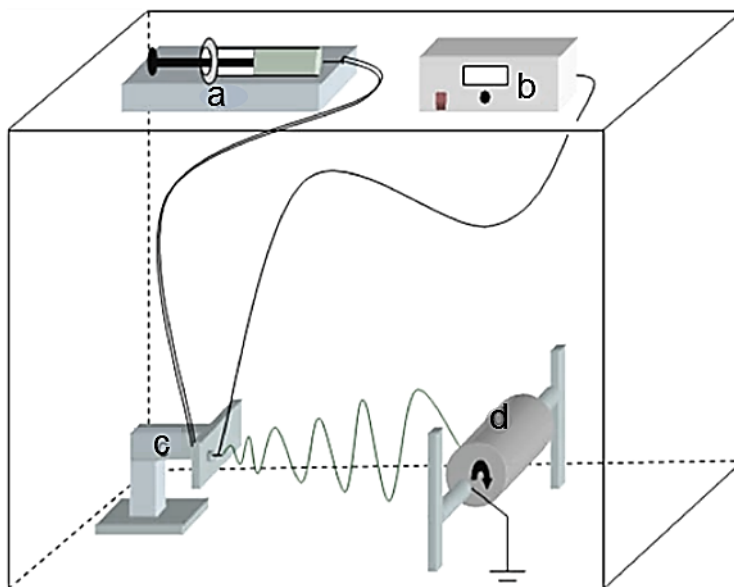
72 The control membrane used in this work was CTA forward osmosis membrane. This membrane was
73 provided by Hydration Technology Innovations (HTI) Water Technology (Albany, OR) which is widely
74 applied for a number of FO applications, such as seawater desalination (Linares et al., 2017), wastewater
75 treatment (Al-Furaiji et al., 2019), and advanced life support systems (Cath et al., 2005). Properties and
76 images of the membrane can be found elsewhere (McCutcheon et al., 2005).

77 **2.2. PAN nanofiber and PES support layers fabrication**

78 PAN nanofibers were prepared using a custom-built electrospinning setup (Figure 1). The electrospinning
79 setup contained a high voltage power supply, a syringe pump, and a rotating drum. The syringe pump was
80 made from locally available parts. A grounded aluminum rotating drum, which served as a collector, was
81 placed at a distance of 15 cm from the needle's tip, and an electrical potential was used at a voltage of 30
82 kV using the power supply device.

83 The solution of PAN in DMF was prepared by continuously stirring the polymer in the solvent for 24 h
84 at 60°C. After obtaining the desired solution, it was left to cool and degas overnight at room temperature
85 prior to electrospinning. The as-prepared polymeric solution was electrospun at a flow rate of 1 mL/h
86 onto an aluminum foil which is peeled off before using the membrane in preparing the TFC membranes.
87 Electrospinning was conducted at ambient temperature and humidity.

88 In order to compare the mechanical properties of the prepared support layer with a common support layer
89 used for the same purpose, a polyethersulfone support sheet was prepared via the phase inversion
90 phenomenon. 15% PES was dissolved in DMF by applying heat and stirring for 3 h until a colorless
91 solution formed without any polymer residue. After maintaining the solution at 60 °C during heating, it
92 was left to cool at room temperature overnight for degassing. The solution was extended on a glass plate
93 via a home-made casting knife to a thickness of 130 μm and immersed in a water bath. The solution
94 turned to a white sheet and separated from the glass in a few seconds. The sheet was rinsed with water
95 three times before storing and use.



97

98 **Figure 1 A diagram of the custom-built Electrospinning setup, (a) syringe pump, (b) high voltage supply, (c)**
99 **transition stage, and (d) rotating collector.**

100

101 **2.3. Interfacial Polymerization to Make TFC Membrane.**

102 The TFC membranes were prepared via the interfacial polymerization reaction at the interface between
103 MPD aqueous solution and TMC organic solution. 2% of MPD was dissolved in DI water to prepare the
104 aqueous solution, while the organic solution was prepared by dissolving 0.15% of TMC in isooctane. The
105 IP reaction was conducted on the PAN support layer as follows: First, the as-spun PAN was mounted on
106 a glass plate and the MPD solution was poured on its top and kept in contact with the PAN support sheet
107 for 60 s (Kadhom et al., 2016). The excess of the solution was ejected using a squeegee ruler. Then, the
108 TMC solution was poured on the PAN sheet that contained the MPD active sites and kept in contact for
109 30 s. The resulting TFC membrane was then dried for 10 min at 60°C and stored in DI water prior to the
110 performance examination.

111

112

2.4. Membranes Characterizations

The Morphology analysis of the prepared membranes was determined using a Scanning Electron Microscope (SEM, VEGA3 - TESCAN, Czechoslovakia). The mechanical properties of the different membranes were obtained from the tensile tests in the air at 25 °C using an Instron microforce tester. A dynamic mechanical analysis (DMA) controlled force module was selected and a minimum of three strips (with a size of 40 mm x 5.5 mm) were tested from each type of membrane. The porosity of the membranes was estimated using the gravimetric method. The membrane was cut as disks with a diameter of 2.54 cm (1 in) and weighed (W_{dry}). Isopropyl alcohol (IPA) was used as a wetting agent and the membrane weighed after immersed in IPA (W_{wet}). The porosity (ε) was calculated from the following equation:

$$\varepsilon = \frac{\left(\frac{W_{wet} - W_{dry}}{\rho_{IPA}} \right)}{V} \times 100\%$$

where ρ_{IPA} is the density of IPA and V is the total volume of the sample. Each membrane was tested at least three times. The membranes' wettability was studied by measuring the contact angle (Theta Lite TL-101 Thailand).

2.5. Forward osmosis performance tests

The FO tests were carried out using the experimental set-up illustrated in Figure 2. The installation consists of two tanks: one was specified for the feed solution, while the other was for the draw solution. Both solutions were pumped to the membrane cell using diaphragm pumps from Pure-water®. The membrane was installed in a custom-made cell with dimensions of 7.62 cm length, 2.54 cm width, and 0.3 cm depth. The selection of the feed and draw solutions was according to the standard methodology described by Cath et al. 2013. The DI water was used as a feed solution while 1 M NaCl solution was used as a draw solution. The water permeation flux was estimated as follows:

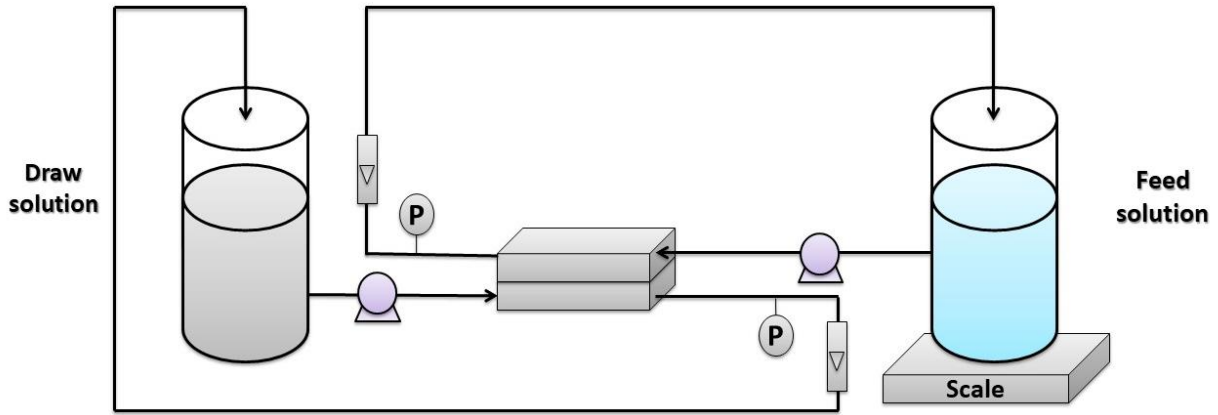
$$J_w = \frac{\Delta w}{\rho A t}$$

Where J_w is the water flux ($\text{Lm}^{-2}\text{h}^{-1}$), Δw represents the difference in the feed solution weight (g), ρ is water density at operating temperature (g/L), A is the actual operative area of the membrane ($20 \times 10^{-4} \text{ m}^2$), and t is the experiment time.

138 Solute flux through the membrane was estimated by monitoring the conductivity of the feed solution and
139 using the following equation:

$$140 J_s = \frac{\Delta CV}{At}$$

141 Where J_s represents the solute flux ($\text{gm}^{-2}\text{h}^{-1}$), ΔC is the change in feed solution concentration (g/L)
142 (calculated from the conductivity change), and V stands for the volume of feed solution (L).



143

144

Figure 2 Schematic diagram of the FO bench-scale test unit.

145

3. Results and Discussion

146

3.1. Membrane characterization

147

148

149

150

151

152

153

154

155

Figure 3 illustrates the SEM images of the PAN's support layer that was prepared by the electrospinning technique. It can be observed that the membrane is structured of smooth and uniform fibers with an approximate diameter of 250 nm. The cross-sectional SEM image (Figure 4) shows that the membrane consists of nanofibrous layers with a thickness of about 75 microns. It can also be noticed that the underlying nanofibers own a very high porosity on their surfaces. This could assure maximum contact between PAN nanofibers with the draw solution during the forward osmosis operation, which means higher mass transfer area and consequently higher water flux. Figure 5 illustrates the surface morphology of the PAN nanofiber membrane after the interfacial polymerization reaction. Also, it can be seen that the polyamide selective membrane was successfully formed on the PAN nanofiber support sheet. It can be

156 seen from the SEM image after the IP reaction that it has a leaf-like morphology compared to the PAN
157 support layer which has a nanofibrous structure. It was reported in the literature that the leaf-like structure
158 confirms the formation of the polyamide selective layer. The contact angle measurement of the prepared
159 membranes showed that it has a hydrophilic surface with an average contact angle of 35°. The
160 hydrophilicity of the membrane's surface is an important factor in the osmotically driven membrane
161 processes (Darwish et al., 2020). This could be explained as the solutes can exclusively diffuse within the
162 wetted area of the support sheet. Ultimately, the unsaturated parts inside the internal structure of the
163 support layer couldn't be calculated as an actual mass transfer area. As much as the internal surfaces of
164 the pores and inner vacancy get wet, the porous support layer can contribute to producing a membrane
165 with a better osmotic water flux performance.

166 **3.2. Support sheet mechanical properties and porosity**

167 3.2.1 Mechanical properties

168 Using a support layer for the TFC membrane that usually applied in nanofiltration, reverse
169 osmosis, and forward osmosis is inevitable due to the tiny thickness of the active membrane. The support
170 layer was found to significantly affect the total performance and commonly made of polymers. Many
171 factors could influence layer usage such as its raw material, method and conditions of preparation, doping
172 additives, porosity, tortuosity, etc (Kadhom and Deng, 2018). In most cases, the support layer is
173 manufactured using the phase inversion phenomenon for a low hydrophilicity polymer. In this work, a
174 PAN layer was synthesized using the electrospinning, which is expected to produce higher internal
175 porosity than the sheets produced via phase inversion. Therefore, the mechanical properties were studied
176 and compared to the commonly used support layer produced by phase inversion.

177 Figure 6 shows the relation between the stress and strain of the PAN sheet. It can be observed
178 that the maximum stress was 1.258 MPa, which was associated with the strain of 15.31%. When these
179 values were compared with 15% Polyethersulfone support sheet (as an example of the familiarly applied
180 support layers), the stress is lower but the strain is higher. The measured stress and strain of the PES
181 sheet were around 2.45 MPa and 8.7%, respectively. It can be noted that the PAN sheets had a lower

182 mechanical strength but a higher elongation rate. This result is expected due to the method of preparation,
183 wherein the electrospinning the nanofibers are made individually and connect with each other on the
184 rotating cylinder. While in the phase inversion, the sheet formed by stiffening the polymer and discarding
185 the solvent. The average values of other mechanical properties were listed in Table 1 with the standard
186 deviation of three measurement values.

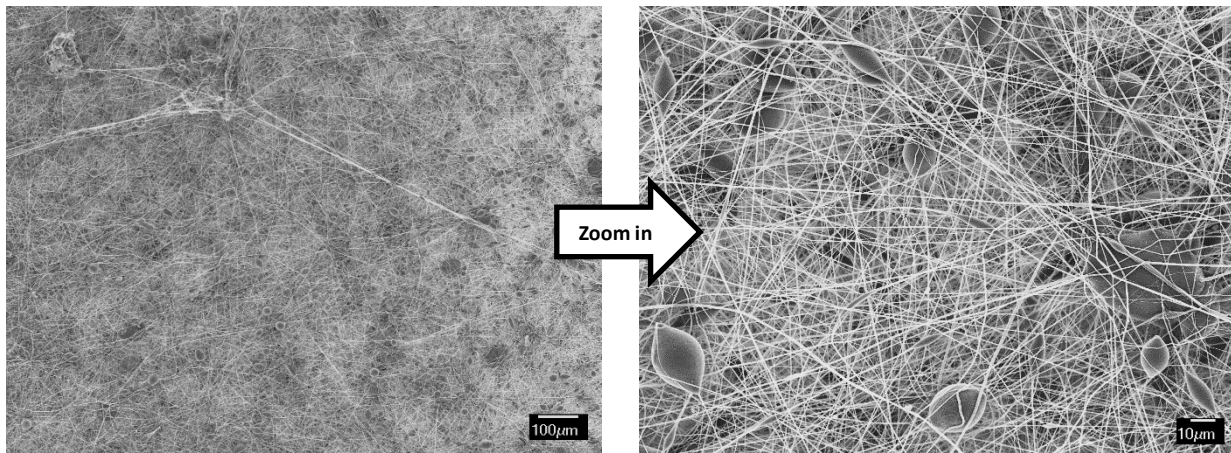
187 **Table 1. Mechanical properties of PAN support layer**

Mechanical Property	Average value	Standard deviation	Units
Young's modulus	9.4065	1.0288	MPa
Tensile strength	1.3586	0.1428	MPa
Elongation at break	17.8463	3.5857	(%)

188

189 3.2.2 Porosity

190 PAN support layer was prepared by the electrospinning to achieve a high porosity. However, the
191 average porosity values of the PAN and classic PES layers were 92.07% \pm 2.09 and 60.0% \pm 1.53,
192 respectively. From these values, it can be seen that the PAN sheet is more porous than the PES sheet.
193 This could help in penetrating the water and, anyway, solute through the membrane structure, which could
194 improve the water flux. Higher porosity means lower unreach spaces and dead ends.

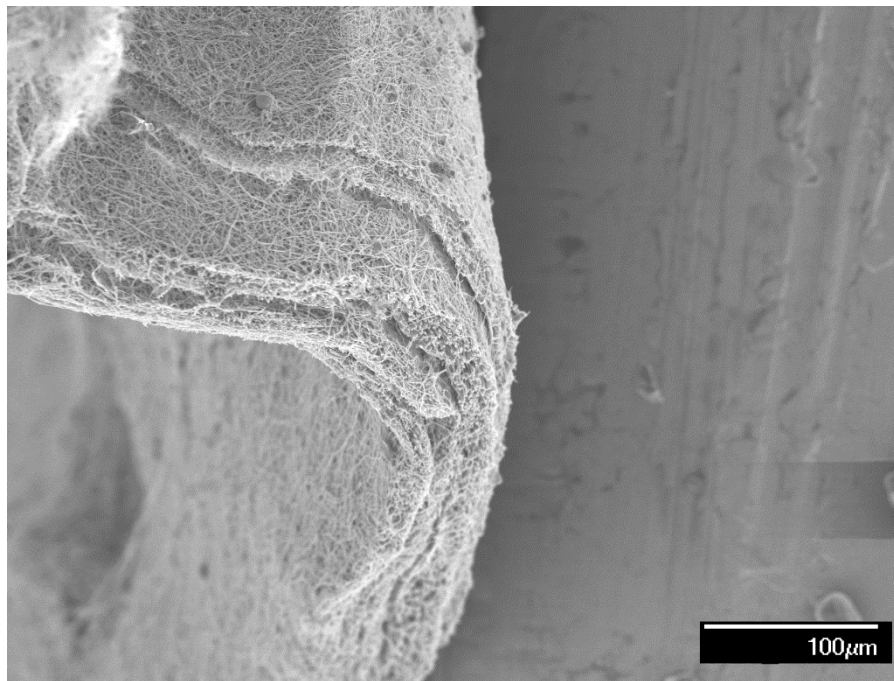


195

196

197

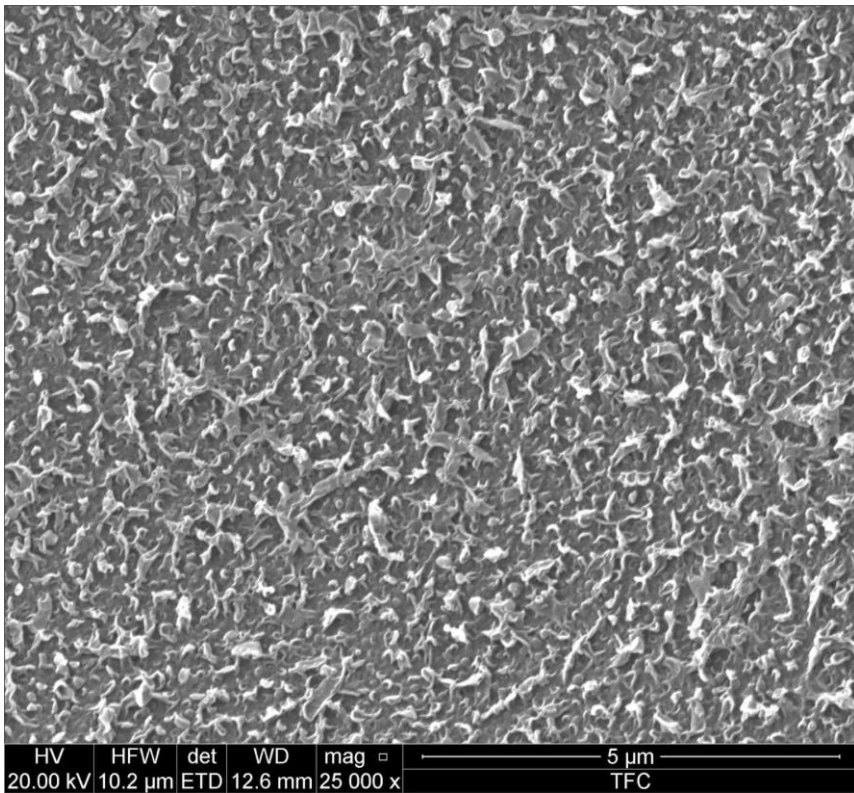
Figure 3 Surface SEM images of the as-spun PAN nanofiber mat.



198

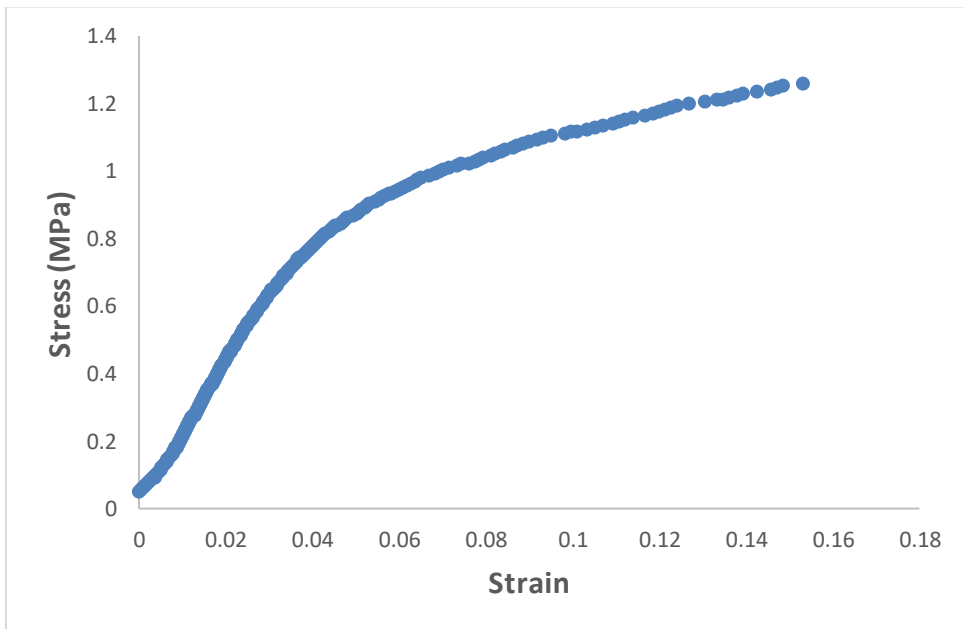
199

Figure 4 Cross-sectional SEM image of the as-spun PAN nanofiber mat.



200

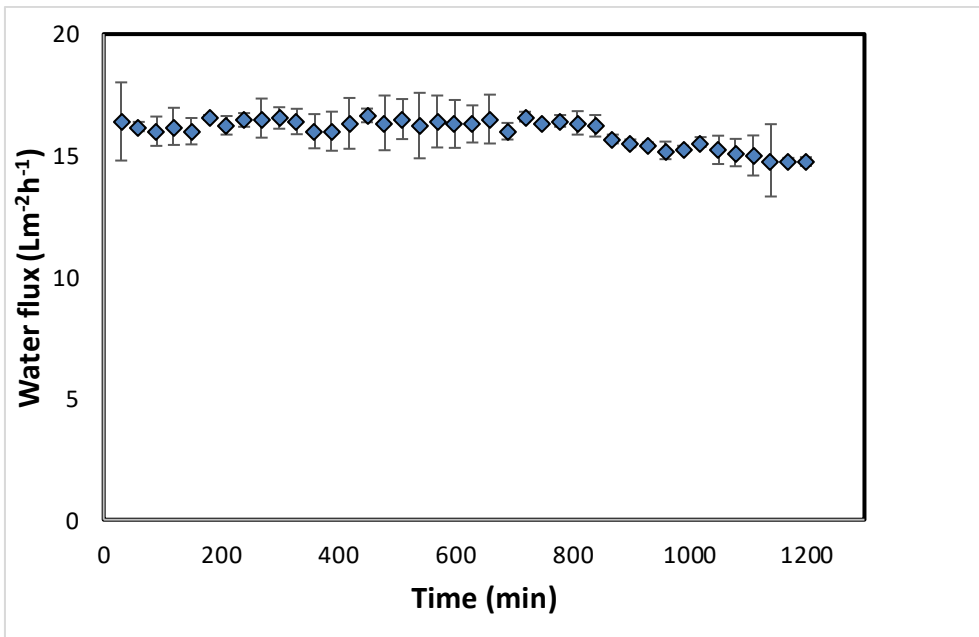
Figure 5 Surface SEM image of the TFC PAN membrane.



201

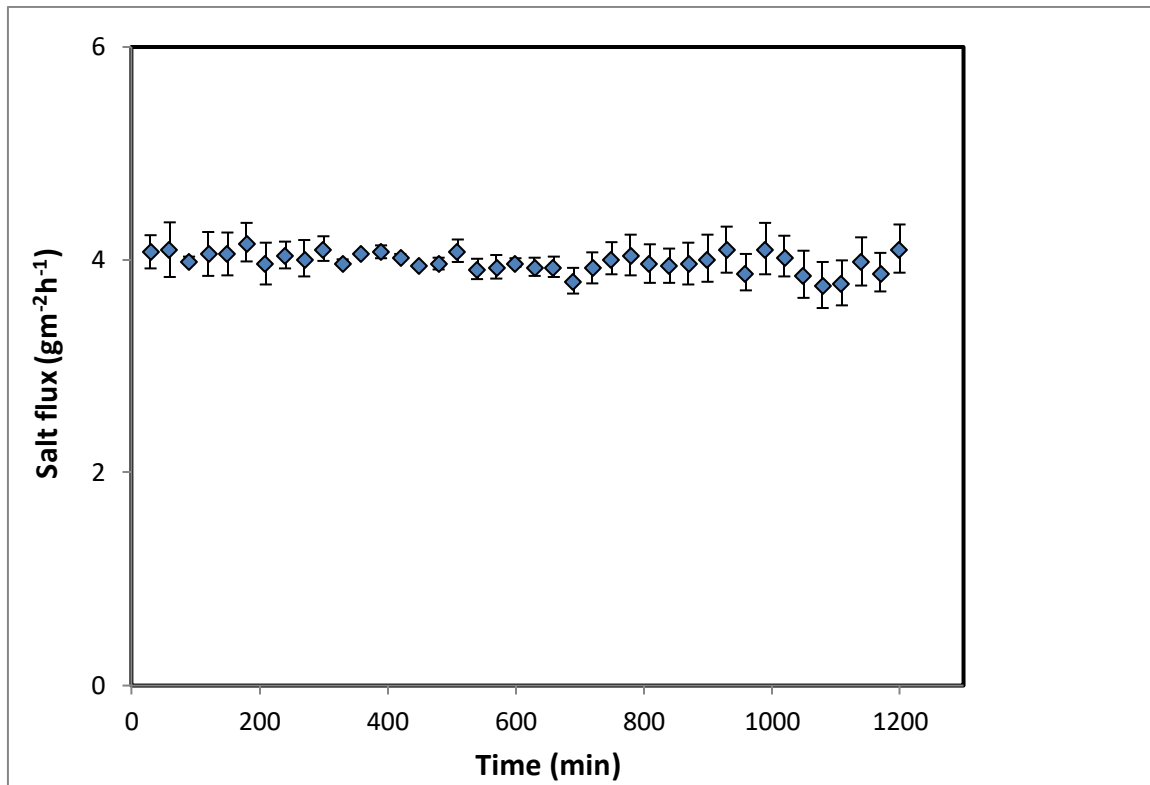
203 3.3. Membrane performance in FO operation

204 The osmotic efficiency of the TFC membrane supported by the nanofiber layer was examined using DI
205 water as a feed solution, whereas 1 M NaCl solution was used as a draw solution according to the
206 standard methodology for testing the osmotically driven membranes (Cath et al., 2013). Results of water
207 flux and salt reverse flux are clarified in Figures 7 and 8, respectively. PAN-TFC membrane showed a
208 stable flux of about 16 LMH for 20 h of operation. Reverse salt flux exhibited similar behavior with an
209 average value of about 4 GMH. In order to compare the performance of the PAN-TFC membrane with
210 commercial membranes, we tested CTA membranes from HTI under the same operating conditions, the
211 results were illustrated in Figure 9. Also, a comparison of the PAN-TFC membrane with some of the
212 commercially available FO membranes can be found in Table 2. It can be distinguished from the figure
213 that the PAN-TFC membrane's water flux was higher than the HTI-CTA membrane's water flux. This
214 could be attributed to the highly porous surface structure of the nanofiber support layer for the PAN-
215 TFC membrane; this porous surface generates a more effective mass transfer area, and consequently
216 higher water flux. However, the reverse salt flux of the commercial membrane was lower compared to
217 the PAN-TFC membrane. This could ascribe to its better mechanical strength and rigidity compared with
218 the nanofibrous composite membranes, which commonly have modest mechanical properties.
219 Nevertheless, the FO applications are famous to have low or no hydraulic pressure required to drive the
220 process; here, it can result that the osmotic efficiency of the membrane is more important than its rigidity.



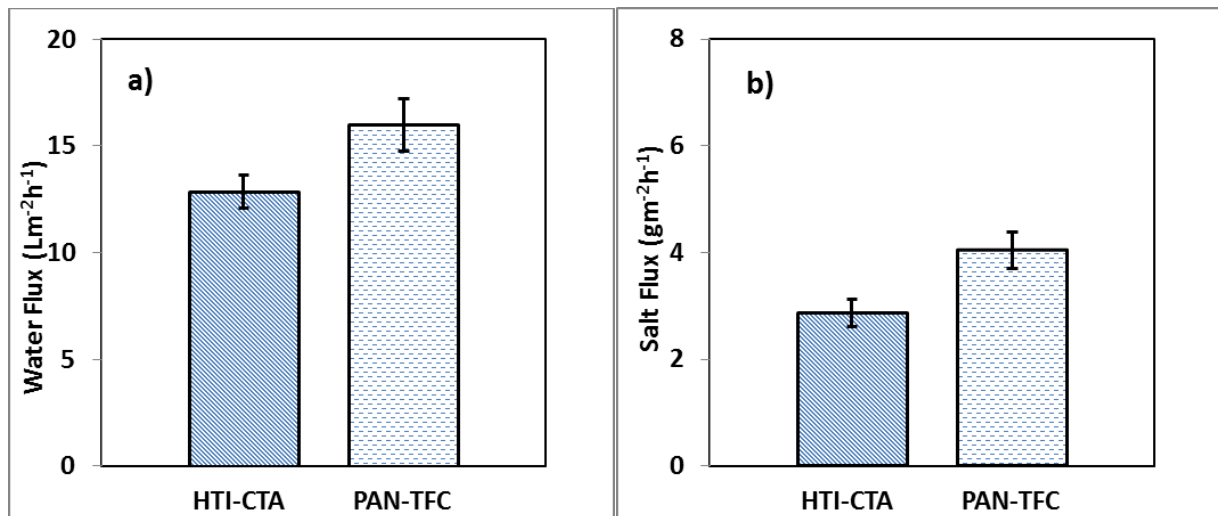
221

222 **Figure 7 Forward osmosis water flux for the PAN-TFC membrane. Experimental conditions: feed solution: DI water,**
223 **draw solution: 1 M NaCl, FO mode, volumetric flow-rate of feed and draw 0.6 L/min, Temp 25° C, zero transmembrane**
224 **pressure. Results are an average of three experiments with different coupons. Error bars indicate standard deviation.**



225

226 **Figure 8 Forward osmosis salt flux for the PAN-TFC membrane. Experimental conditions: feed solution: DI water,**
 227 **draw solution: 1 M NaCl, FO mode, volumetric flow-rate of feed and draw 0.6 L/min, temp 25° C, zero transmembrane**
 228 **pressure. Results are an average of three experiments with different trails. Error bars indicate standard deviation.**



229

230 **Figure 9 Forward osmosis water flux and salt flux for the PAN-TFC membrane. Experimental conditions: feed**
231 **solution: DI water, draw solution: 1 M NaCl, FO mode, volumetric flow-rate of feed and draw 0.6 L/min, temp 25° C,**
232 **zero transmembrane pressure. Results are an average of three experiments with different coupons. Error bars indicate**
233 **standard deviation.**

234 **Table 2 Performance of some of the commercially FO membranes.**

Membrane	Feed Solution	Draw Solution	Water Flux	Salt Flux	Reference
PAN-TFC	DI	1 M NaCl	16	4	This work
HTI-TFC	DI	1 M NaCl	15	4.5	(Ren and McCutcheon, 2018)
Aquaporin TFC	DI	1 M NaCl	9	4	(Xia et al., 2017)
Oasys TFC	DI	1 M NaCl	30	50	(Cath et al., 2013)
Porifera CTA	DI	1 M NaCl	29		(Roy et al., 2016)

235

236 **4. Conclusions and Recommendations**

237 TFC membrane with a fibrous structure was prepared in this research and tested for forward osmosis
238 application. The electrospinning setup was made from locally available parts. This system exhibited stable
239 operation in making the electrospun nanofiber membrane. The prepared TFC membrane showed good
240 performance in terms of water flux and salt rejection. TFC-PAN membranes showed a stable water flux
241 with an average value of 16 LMH comparing to the CTA commercial membranes with 13 LMH water
242 flux. Future research can focus on incorporating specific nanoparticles to enhance membranes'
243 performance. Also, studying the exposure time of MPD and TMC on the performance of the membrane
244 is highly recommended.

245 **Acknowledgment**

246 The authors like to thank their affiliations, the ministry of science and technology, Alkarkh University of
247 Science, University of Baghdad, and University of Wasit, for partially supporting this work.

248 **Funding**

249 The authors received no fund.

250 **Conflicts of Interest**

251 The authors declare no conflicts of interest.

252 **References**

- 253 Al-Furaiji, M., Benes, N., Nijmeijer, A., McCutcheon, J.R., 2019. Use of a Forward Osmosis–
254 Membrane Distillation Integrated Process in the Treatment of High-Salinity Oily Wastewater. *Ind.*
255 *Eng. Chem. Res.* 58, 956–962. <https://doi.org/10.1021/acs.iecr.8b04875>
- 256 Al-Furaiji, M.H.O., Arena, J.T., Chowdhury, M., Benes, N., Nijmeijer, A., McCutcheon, J.R., 2018.
257 Use of forward osmosis in treatment of hyper-saline water. *Desalin. Water Treat.* 133, 1–9.
258 <https://doi.org/10.5004/dwt.2018.22851>
- 259 Ang, W.L., Wahab Mohammad, A., Johnson, D., Hilal, N., 2019. Forward osmosis research trends in
260 desalination and wastewater treatment: A review of research trends over the past decade. *J. Water*
261 *Process Eng.* 31, 100886. <https://doi.org/10.1016/j.jwpe.2019.100886>
- 262 Bui, N.N., McCutcheon, J.R., 2013. Hydrophilic nanofibers as new supports for thin film composite
263 membranes for engineered osmosis. *Environ. Sci. Technol.* 47, 1761–1769.
264 <https://doi.org/10.1021/es304215g>
- 265 Cath, T.Y., Adams, D., Childress, A.E., 2005. Membrane contactor processes for wastewater
266 reclamation in space: II. Combined direct osmosis, osmotic distillation, and membrane distillation
267 for treatment of metabolic wastewater. *J. Memb. Sci.* 257, 111–119.
268 <https://doi.org/10.1016/j.memsci.2004.07.039>
- 269 Cath, T.Y., Childress, A.E., Elimelech, M., 2006. Forward osmosis: Principles, applications, and recent
270 developments. *J. Memb. Sci.* 281, 70–87. <https://doi.org/10.1016/j.memsci.2006.05.048>
- 271 Cath, T.Y., Elimelech, M., McCutcheon, J.R., McGinnis, R.L., Achilli, A., Anastasio, D., Brady, A.R.,
272 Childress, A.E., Farr, I. V., Hancock, N.T., Lampi, J., Nghiem, L.D., Xie, M., Yip, N.Y., 2013.
273 Standard Methodology for Evaluating Membrane Performance in Osmotically Driven Membrane

274 Processes. *Desalination* 312, 31–38. <https://doi.org/10.1016/j.desal.2012.07.005>

275 Chowdhury, M.R., Huang, L., McCutcheon, J.R., 2017. Thin Film Composite Membranes for Forward
276 Osmosis Supported by Commercial Nanofiber Nonwovens. *Ind. Eng. Chem. Res.* 56, 1057–1063.
277 <https://doi.org/10.1021/acs.iecr.6b04256>

278 Darwish, N. Bin, Alkudhiri, A., AlRomaih, H., Alalawi, A., Leaper, M.C., Hilal, N., 2020. Effect of
279 lithium chloride additive on forward osmosis membranes performance. *J. Water Process Eng.* 33,
280 101049. <https://doi.org/10.1016/j.jwpe.2019.101049>

281 Huang, L., McCutcheon, J.R., 2014. Hydrophilic nylon 6,6 nanofibers supported thin film composite
282 membranes for engineered osmosis. *J. Memb. Sci.* 457, 162–169.
283 <https://doi.org/10.1016/j.memsci.2014.01.040>

284 Kadhom, M., Deng, B., 2019. Synthesis of high-performance thin film composite (TFC) membranes by
285 controlling the preparation conditions: Technical notes. *J. Water Process Eng.* 30, 100542.
286 <https://doi.org/10.1016/j.jwpe.2017.12.011>

287 Kadhom, M., Yin, J., Deng, B., 2016. A thin film nanocomposite membrane with MCM-41 silica
288 nanoparticles for brackish water purification. *Membranes (Basel)*. 6.
289 <https://doi.org/10.3390/membranes6040050>

290 Linares, R.V., Li, Z., Elimelech, M., Amy, G., Vrouwenvelder, H., 2017. Recent Developments in
291 Forward Osmosis Processes. *Water Intell. Online*. <https://doi.org/10.2166/9781780408125>

292 McCutcheon, J.R., McGinnis, R.L., Elimelech, M., 2005. A novel ammonia-carbon dioxide forward
293 (direct) osmosis desalination process. *Desalination* 174, 1–11.
294 <https://doi.org/10.1016/j.desal.2004.11.002>

295 Ren, J., McCutcheon, J.R., 2018. A new commercial biomimetic hollow fiber membrane for forward
296 osmosis. *Desalination* 442, 44–50. <https://doi.org/10.1016/j.desal.2018.04.015>

297 Ren, J., McCutcheon, J.R., 2014. A new commercial thin film composite membrane for forward
298 osmosis. *Desalination* 343, 187–193. <https://doi.org/10.1016/j.desal.2013.11.026>

299 Roy, D., Rahni, M., Pierre, P., Yargeau, V., 2016. Forward osmosis for the concentration and reuse of
300 process saline wastewater. *Chem. Eng. J.* 287, 277–284. <https://doi.org/10.1016/j.cej.2015.11.012>

301 Waisi, B.I., Manickam, S.S., Benes, N.E., Nijmeijer, A., McCutcheon, J.R., 2019. Activated Carbon

302 Nanofiber Nonwovens: Improving Strength and Surface Area by Tuning Fabrication Procedure.
303 Ind. Eng. Chem. Res. 58, 4084–4089. <https://doi.org/10.1021/acs.iecr.8b05612>
304 Xia, L., Andersen, M.F., Hélix-Nielsen, C., McCutcheon, J.R., 2017. Novel Commercial Aquaporin
305 Flat-Sheet Membrane for Forward Osmosis. Ind. Eng. Chem. Res. 56, 11919–11925.
306 <https://doi.org/10.1021/acs.iecr.7b02368>

307

308